Clim. Past Discuss., 7, 1845–1886, 2011
www.clim-past-discuss.net/7/1845/2011/
doi:10.5194/cpd-7-1845-2011

Climate of the Past Discussions

Deglaciation records of ^{17}O-*excess* in East Antarctica: reliable reconstruction of oceanic relative humidity from coastal sites

R. Winkler[1], A. Landais[1], H. Sodemann[2], L. Dümbgen[3], F. Prié[1], V. Masson-Delmotte[1], B. Stenni[4], and J. Jouzel[1]

[1]Laboratoire des Sciences du Climat et de l'Environnement (LSCE/IPSL/CEA/CNRS/UVSQ), UMR8212, Orme des Merisiers, 91191 Gif-sur-Yvette, France
[2]Institute for Atmospheric and Climate Science, Swiss Federal Institute of Technology Zürich, Universitätsstrasse 16, 8092 Zürich, Switzerland
[3]Department of Mathematics and Statistics, Institute of Mathematical Statistics and Actuarial Science, University of Bern, Alpeneggstrasse 22, 3012 Bern, Switzerland
[4]Department of Geosciences, University of Trieste, Via E. Weiss 4, 34127 Trieste, Italy

Received: 20 May 2011 – Accepted: 29 May 2011 – Published: 10 June 2011

Correspondence to: R. Winkler (renato.winkler@lsce.ipsl.fr)

Published by Copernicus Publications on behalf of the European Geosciences Union.

Abstract

We measured $\delta^{17}O$ and $\delta^{18}O$ in two Antarctic ice cores at EPICA Dome C (EDC) and TALDICE (TD), respectively and computed ^{17}O-*excess* with respect to VSMOW. The comparison of our ^{17}O-*excess* data with the previous record obtained at Vostok (Landais et al., 2008) revealed differences up to 35 ppm in ^{17}O-*excess* mean level and evolution for the three sites. Our data showed that the large increase depicted at Vostok (20 ppm) during the last deglaciation, is a regional and not a general pattern in the temporal distribution of ^{17}O-*excess* in East Antarctica. The EDC data display an increase of 13 ppm, whereas the TD data show no significant variation from the Last Glacial Maximum (LGM) to the Early Holocene (EH). Lagrangian moisture source diagnostic revealed very different source regions for Vostok and EDC compared to TD. These findings combined with the results of a sensitivity analysis, using a Rayleigh-type isotopic model, suggest that relative humidity (RH) at the oceanic source region (OSR) are a determining factor for the spatial differences of ^{17}O-*excess* in East Antarctica. However, ^{17}O-*excess* in remote sites of continental Antarctica (e.g. Vostok) may be highly sensitive to local effects. Hence, we consider ^{17}O-*excess* in coastal East Antarctic ice cores (TD) to be more reliable as a proxy for RH at the OSR.

1 Introduction

1.1 Stable water isotopes in the hydrological cycle

The stable isotopes $^{2}H/H$ and $^{18}O/^{16}O$ ratios of water molecules in ice cores have been used for several decades as proxies for past temperature over the polar regions and have permitted to reconstruct past climate changes over the last 800 ka (ka = thousand years before present) in Antarctica (Jouzel et al., 2007). Their link with temperature results from isotopic fractionation of water at each phase transition in the water cycle and especially along the water mass trajectory from the region of evaporation to the

CPD
7, 1845–1886, 2011

polar regions of final precipitation. The combination of δ^2H and δ^{18}O leads to the second order parameter d-*excess* = δ^2H – 8 δ^{18}O (Dansgaard, 1964). It has been shown that d-*excess* in ice/snow from polar regions is mainly a function of temperature at the oceanic moisture source region (OSR) (Ciais and Jouzel, 1994), (Petit et al., 1991), but it also depends on relative humidity (RH) at the OSR (Jouzel et al., 1982), the surface ocean isotopic composition, wind speed and finally the temperature at the precipitation site (e.g. Stenni et al., 2001 and 2010; Vimeux et al., 2002). The dependence of d-*excess* with these different parameters is variable from one site to another (Masson-Delmotte et al., 2008; Vimeux et al., 1999) and it is thus difficult to infer quantitative information on climatic conditions at the evaporative regions from d-*excess* alone.

Angert et al. (2004) suggested that another second order parameter provided by the combination of δ^{17}O and δ^{18}O in ^{17}O-*excess* = $\ln(\delta^{17}\mathrm{O}+1) - 0.528 \cdot \ln(\delta^{18}\mathrm{O}+1)$ of ice cores would provide additional information on humidity conditions of the OSR. The expected signal from ^{17}O-*excess* is very small, of the order of 10–40 ppm and thus difficult to measure accurately (in previous studies (e.g. Luz et al., 1999) the unit "permeg" instead of ppm was used. In order to be consistent with the SI system (Kaiser, 2011) we use ppm instead of permeg). Progress in analytical devices have allowed Barkan and Luz (2005) to measure δ^{17}O and δ^{18}O with a sufficiently high precision to calculate ^{17}O-*excess* of water samples. Their laboratory study also showed that ^{17}O-*excess* should not depend on OSR temperature. Extending the theoretical approach developped by (Craig and Gordon, 1965) and (Merlivat and Jouzel, 1979) to link d-*excess* and conditions prevailing at the OSR, one can derive that ^{17}O-*excess* and RH of the OSR are linearly related with decreasing ^{17}O-*excess* for increasing RH. This expected negative correlation has recently been monitored in situ (surface water vapour) over the Southern Ocean by Uemura et al. (2010).

Landais et al. (2008) identified an increase of ^{17}O-*excess* from 20 to 40 ppm between the Last Glacial Maximum (LGM, 21 ka) and Early Holocene (EH, 8 ka) in the Vostok ice core in East Antarctica. They attributed this 20 ppm increase to a decrease in RH of 20 % over the Vostok OSR. However a 20 % decrease in RH over the ocean (from

CPD
7, 1845–1886, 2011

LGM to EH) appears large and is not supported by atmospheric general circulation models, which simulate unchanged ocean surface RH over glacial/interglacial periods (Risi et al., 2010).

The work of Landais et al. (2008) raised the question if the deglacial increase at Vostok in ^{17}O-*excess* is a local signal or if it is a more regional pattern that could be observed at other sites in Antarctica. Here, we address this question by analysing the temporal variations of ^{17}O-*excess* over the last deglaciation (21 to 8 ka) at two other sites in East Antarctica with very different climatic conditions: EPICA Dome C (EDC) and Talos Dome (TD).

The ice cores of EDC and TD provide both continuous high quality information about the past climate. EDC (75°06′ S, 123° E) is characterised by continental climatic conditions (modern annual mean temperature: −54.5 °C) and a very low accumulation rate of about 25 kg m$^{-2}a^{-1}$. The geographical location and the climatic conditions at the drilling site of EDC are comparable to those at Vostok (78° 27′ S, 106° 50′ E) although Vostok is slightly colder and drier, with a temperature of −55.3 °C and an accumulation rate of about 21.5 kg m$^{-2}a^{-1}$ (Masson-Delmotte et al., 2011). TD (72° 49′ S, 159° 11′ E) is situated in the coastal area of East Antarctica and is marked by higher temperature (−40.1 °C) and much higher accumulation rate of 80 kg m$^{-2}a^{-1}$ (Stenni et al., 2011).

In this article, we first give a short summary of the definitions used for the triple isotopic composition of oxygen in water as well as an overview of the different fractionation effects in the hydrological cycle. Then, we present the ^{17}O-*excess* profiles obtained on the EDC and TD ice cores. A statistical analysis is performed to test the significance of glacial/interglacial shifts. To help with the interpretation of the different water isotopic profiles, we use the classical simple isotopic model adapted to the description of water isotopes in Antarctica (Mixed Cloud Isotopic Model, hereafter MCIM – Ciais and Jouzel, 1994). We perform sensitivity studies with various configurations of the supersaturation parameter of the MCIM to discuss the different influences on ^{17}O-*excess* on coastal and continental East Antarctic ice cores over the last deglaciation.

CPD
7, 1845–1886, 2011

2 Fractionation processes in the triple isotopic composition of oxygen in meteoric water

2.1 Equilibrium fractionation

During each phase-change in the water cycle, fractionation of stable water isotopes occurs. Two different kinds of fractionation are distinguished. The first one is called equilibrium fractionation: for water molecules containing heavy oxygen or hydrogen isotopes the water vapour pressure is lower than for the abundant (light) water molecules. For this reason water molecules which contain ^{17}O, ^{18}O or deuterium stay preferably in the condensed phase compared to the lightest $H_2^{16}O$ molecules. To quantify isotopic fractionation, the equilibrium fractionation factor α_{eq} has been introduced. α_{eq} varies with temperature and was theoretically determined for the different water isotopes by Van Hook (1968). α_{eq} for $\frac{H_2^{18}O}{H_2^{16}O}$ was measured for ice-vapour and for liquid-vapour by Majoube (1971a,b), for temperatures between 0 and −33 °C . The ratios of $\frac{H^2H^{16}O}{H_2^{16}O}$ were measured by Merlivat and Nief (1967) for the temperature range of 0 to −40 °C for ice-vapour and from 0 to −15 °C for liquid-vapour. α_{eq} for $\frac{H_2^{17}O}{H_2^{16}O}$ has been measured by Barkan and Luz (2005) for liquid – vapour over the temperature range of 11.4 to 41.5 °C.

2.2 Kinetic fractionation

The second kind of fractionation is due to the different molecular diffusivities and is called kinetic fractionation (Mook, 1994). The fractionation factor for kinetic fractionation α_{kin} is a function of molecular diffusivity D of the considered isotopes. The ratios $^{18}D/^{16}D$ and $^{2}H/^{16}D$ (where ^{18}D and ^{2}H refer to the diffusion constants of the heavy water isotope $H_2^{18}O$ and $^{2}HH^{16}O$ in the gaseous phase, respectively) were measured by Merlivat (1978) and Cappa et al. (2003) who obtained significantly different results.

CPD
7, 1845–1886, 2011

Barkan and Luz (2007) and Luz et al. (2009) confirmed the results of Merlivat (1978) and performed the first experimental measurements of the relative diffusivity of $H_2^{17}O$ vs. $H_2^{16}O$ in air.

2.3 Definition of ^{17}O – *excess*

For a triple isotopic system, the relationship between the isotopic ratios ^{17}R and ^{18}R ($^{*}R = \frac{^{*}O}{^{16}O}$, * referring to ^{17}O or ^{18}O, respectively) is governed by a power law (Eq. 1) (Mook and Grootes, 1973), (Craig, 1957):

$$\frac{^{17}R_s}{^{17}R_r} = \left(\frac{^{18}R_s}{^{18}R_r}\right)^{\lambda} \quad (1)$$

the subscripts s and r refer respectively to the sample and reference. Starting from Eq. (1), Miller (2002) introduced a logarithmic definition for the ^{17}O -anomaly:

$$\Delta^{17}O = \ln(\delta^{17}O + 1) - \lambda \ln(\delta^{18}O + 1) \quad (2)$$

The advantage of this logarithmic notation is that fractionation lines are straight lines in a $\ln(\delta^{17}O + 1)$ vs. $\ln(\delta^{18}O + 1)$ plot while they are curved in a $\delta^{17}O$ vs. $\delta^{18}O$ plot (Luz and Barkan, 2004). Moreover, although the absolute value of the ^{17}O -anomaly, using the above definition, depends on the isotopic composition of the reference material, the slope λ of the fractionation line in a $\ln(\delta^{17}O + 1)$ vs. $\ln(\delta^{18}O + 1)$ plot does not.
Meijer and Li (1998) analysed the triple isotopic composition of many different natural waters and determined the exponent λ of Eq. (1). They found a value of 0.5281 ± 0.0015. This number seems to be valid for all meteoric waters (Meijer and Li, 1998) and therefore ^{17}O-*excess* was defined by Miller (2002) as:

$$^{17}O - \textit{excess} = \ln(\delta^{17}O + 1) - 0.528 \ln(\delta^{18}O + 1) \quad (3)$$

The number of 0.528 in Eq. (3) is called the slope of the global meteoric waterline for the system of $\ln(\delta^{17}O + 1)$ vs. $\ln(\delta^{18}O + 1)$. An analogy can be drawn with the δ^2H vs. $\delta^{18}O$

CPD
7, 1845–1886, 2011

system where the slope of the global meteoric waterline is 8: $\delta^2H = 8\delta^{18}O + 10‰$ (Craig, 1961) – and leads to d-*excess* definition (d-*excess* $= \delta^2H - 8\delta^{18}O$) (Dansgaard, 1964).

2.4 Evaporation

During the process of evaporation over the ocean, equilibrium and kinetic fractionation contribute simultaneously to the lower value of $\delta^{17}O$ and $\delta^{18}O$ of the water vapour with respect to $\delta^{17}O$ and $\delta^{18}O$ of the ocean. The ratio between the fractionation factors differs for equilibrium fractionation ($\ln{}^{17}\alpha_{eq}/\ln{}^{18}\alpha_{eq} = 0.529$) and for kinetic fractionation ($\ln\frac{^{17}D}{^{16}D}/\ln\frac{^{18}D}{^{16}D} = 0.518$). Relatively stronger kinetic fractionation leads to an increase of ^{17}O-*excess* in the water vapour. The relative contribution of kinetic fractionation to the total fractionation process at evaporation is negatively correlated to RH at the site of evaporation. As a consequence, variations of ^{17}O-*excess* in the evaporate over the ocean surface are directly related to changes in RH at the ocean surface with:

$$^{17}O - excess = -\ln({}^{18}\alpha_{eq}^{0.529}({}^{18}\alpha_{diff}^{0.518}(1 - RH_n) + RH_n)) + 0.528\ln({}^{18}\alpha_{eq}(\alpha_{diff}(1 - RH_n) + RH_n)) \quad (4)$$

where the exponent-coefficients of 0.518 and 0.529, are respectively based on the experiments of Barkan and Luz (2005, 2007). ${}^{18}\alpha_{diff} = (\frac{^{18}D}{^{16}D})^n$, where the exponent n varies between 0 (turbulent wind regime) to 1 (laminar wind regime) (Mook, 1994), (Merlivat and Jouzel, 1979). ${}^{18}\alpha_{diff}$ was determined in wind tunnel experiments by Merlivat and Jouzel (1979) (${}^{18}\alpha_{diff} = 1.006$) and inferred by Uemura et al. (2010) from isotopic measurements in water vapour above the surface of the Southern ocean (${}^{18}\alpha_{diff} = 1.008$). RH_n is the relative humidity normalized at the ocean surface temperature e.g. (Gat and Mook, 1994). Note that a similar influence of RH at evaporation on d-*excess* of the evaporate is predicted because of the strong differences between $({}^{2H}\alpha_{eq} - 1)/({}^{18}\alpha_{eq} - 1)$ (≈ 8) and $(\frac{^{16}D}{^{2H}D} - 1)/(\frac{^{16}D}{^{18}D} - 1)$ (≈ 0.88) when taking the Merlivat (1978) diffusion coefficients.

CPD
7, 1845–1886, 2011

3 Method

3.1 Experimental method

2 µl of water are injected, under a continuous helium flux (20 ml min^{-1}) into a heated (370 °C) nickel-tube, which is filled with CoF_3 where the water-molecule is split into O_2 and hydrofluoric acid (HF). HF is trapped with liquid nitrogen at the exit of the nickel tube. The gaseous O_2 is then trapped in a stainless steel manifold which is immersed in a liquid helium tank. After 40 min of defrosting the manifold is connected to a Dual Inlet Mass-spectrometer (ThermoFisher Delta V) where $\delta^{17}O$ and $\delta^{18}O$ are measured at the same time. Each IRMS measurement contains two runs. During each run, the ratio between the sample and the working standard (O_2-gas) is determined 16 times. We also measure daily our laboratory water-standard, which is calibrated against VSMOW, using the same fluorination- and IRMS-methods. The detailed description of the measurement technique through fluorination and dual inlet mass spectrometry of O_2 is given by Barkan and Luz (2005). The analytical errors associated to each sample (3 to 4 replica) correspond to the pooled standard deviation

$$\sigma_p = \sqrt{\frac{\sum_{i=1}^{k}(n_i - 1)s_i^2}{\sum_{i=1}^{k}(n_i - 1)}} \quad (5)$$

where n_i is the number of replica of the i-th sample (3 to 4), s_i is the standard deviation of the i-th sample and k is the total number of samples. The pooled standard deviation is 6.4 ppm for the 58 EDC data-points and 6.2 ppm for the 44 TD data-points.

Since measurements of ^{17}O-*excess* are of magnitude ppm, small peculiarities of the water fluorination technique or the IRMS may result in significant inter-laboratory offsets. We thus compared working standards spanning the entire range of our measurements between our laboratory (LSCE) and the Institute of Earth Sciences in Jerusalem.

CPD
7, 1845–1886, 2011

The largest difference in ^{17}O-*excess* between the two laboratories were observed for the two extreme standards VSMOW (δ^{18}O = 0 ‰) and Dome F (δ^{18}O = −58.2 ‰). By definition, VSMOW has a ^{17}O-*excess* of 0 ppm. The Dome F internal standard, which is made of surface snow from the site of Dome Fuji in Antarctica (made by Osamu Abe), was measured with ^{17}O-*excess* = 1 ppm at the Institute of Earth Science (Luz and Barkan, 2009) and with a ^{17}O-*excess* of 23 ppm at LSCE. Since the fractionation coefficients associated with δ^{17}O were measured at the Institute of Earth Science, we decided to correct the ^{17}O-*excess* measurements performed at LSCE with respect to the results obtained at the Institute of Earth Science using the inter calibration of our working standards. We will discuss in detail the topic of inter calibration of water standards between different laboratories in a technical paper, which is in preparation.

Figure 1 shows a comparison between measurements performed by Landais et al. (2008) of ^{17}O-*excess* at Vostok over the last deglaciation with 12 new measurements of the same samples conducted at LSCE. Although we compared only a small number of samples, we still depicted an increasing ^{17}O-*excess* trend during the last deglaciation, that corresponds well with the trend observed by Landais et al. (2008). The good comparison of our data points, measured at LSCE with the earlier ones, obtained in Jerusalem, validates our inter calibration and means that the following records obtained at LSCE can be reliably compared to the previous records published in Landais et al. (2008).

3.2 Mixed Cloud Isotopic Model (MCIM)

In order to compare the different mean levels and evolution of ^{17}O-*excess* (and d-*excess*) in continental (Vostok, EDC) and coastal (TD) Antarctic regions we performed several sensitivity experiments with the mixed cloud isotopic model (MCIM) (Ciais and Jouzel, 1994). Among other models (Kavanaugh and Cuffey, 2003; Johnsen et al., 1989; Noone, 2008), we chose this model because up to now, it is one of the most efficient in simulating the evolution of δ^{18}O , d-*excess* and ^{17}O-*excess* in remote

CPD
7, 1845–1886, 2011

Antarctica and thus has been widely used to interpret d-*excess* and $\delta^{18}O$ variations in ice cores (Stenni et al., 2010; Masson-Delmotte et al., 2004; Vimeux et al., 2001; Stenni et al., 2001). This model has been extended to include fractionation factors $^{17}\alpha$ for $H_2{}^{17}O$ and was used by Landais et al. (2008) to interpret the variations of ^{17}O-*excess* over the last deglaciation on the Vostok ice core as a change of RH at the OSR.

The MCIM is based on a Rayleigh distillation (Merlivat and Jouzel, 1979; Jouzel and Merlivat, 1984). It describes the isotopic composition of the condensed phase (liquid water or ice) and the water vapour at each step between the OSR and the precipitation site on the ice sheet. To determine the isotopic composition of the first water vapour over the ocean surface, the assumption that all the evaporated water will return to the ocean as rain ("closure assumption") is made. This assumption is true in nature, but only globally. Locally, one can not assume that all evaporated water will return to the same ocean basin (e.g. Delmotte et al., 2000; Jouzel and Koster, 1996). However, a more sophisticated model study (Risi et al., 2010) using a single column model in the evaporative regions, instead of the closure assumption, showed that the dependency of ^{17}O-*excess* in polar ice with RH remains the same as with the MCIM and could not challenge the interpretation of the ^{17}O-*excess* variations in the Vostok ice core proposed by Landais et al. (2008) with the MCIM.

During the formation of liquid, only equilibrium fractionation occurs. Depending on temperature, the MCIM allows in the zone of "mixed cloud" the coexistence of liquid droplets and ice crystals. In this zone, the Bergeron-Findeisen process associated with kinetic fractionation effects is taken into account (Ciais and Jouzel, 1994). The formation of snow crystals is a non-equilibrium process and the fractionation factor is a function of α_{eq} and α_{kin}:

$$\alpha = \alpha_{eq}\alpha_{kin} \quad (6)$$

CPD
7, 1845–1886, 2011

The relative proportion of kinetic fractionation is governed by the supersaturation function in the cloud, which is (Jouzel and Merlivat, 1984):

$$\alpha_{\text{kin}} = \frac{S}{1 + \alpha_{\text{eq}}(\frac{D}{{}^{*}D})(S-1)} \tag{7}$$

D and ${}^{*}D$ correspond to the diffusion constants for the light and the heavy isotopes, respectively. As in previous studies (Landais et al., 2008; Petit et al., 1991 and Jouzel and Merlivat, 1984) we described S as a linear function of temperature: $S = p + qT_{\text{c}}$, where T_{c} is the temperature in the cloud in °C for every time step of the distillation process. p and q are tunable parameters (see Sect. 4.3).

3.2.1 Forcing and tuning of the MCIM

The model is prescribed by initial parameters such as the temperature, RH , wind speed and pressure of the source region as well as the isotopic composition of the ocean and the condensation temperature (assumed to be linearly related to the surface temperature, Ekaykin and Lipenkov, 2009) and pressure at the precipitation site. There are several tuning parameters (Ciais and Jouzel, 1994) such as the dependence of supersaturation on temperature ($S = p + qT_{\text{c}}$), the fraction of condensate remaining in the cloud, the temperature range where liquid and solid water can coexist, a coefficient (γ) that determines the proportion of the re-evaporation of liquid phase and the parameter, which controls at what temperature the first ice forms. For the tuning of the model, we used a method already used in previous studies (Landais et al., 2008, Masson-Delmotte et al., 2005 Vimeux et al., 1999, 2001 and Stenni et al., 2001; Stenni et al., 2003; Stenni et al., 2010) with δ^{17}O , δ^{18}O and δ^{2}H. We adjusted the tuning parameters to obtain the best simulations of the ^{17}O-*excess* and d-*excess* evolution with δ^{18}O over an Antarctic transect (Terra Nova Bay – Dome C (Landais et al., 2008)). The second constraint for our tuning is to reproduce the δ^{18}O , d-*excess* and ^{17}O-*excess* values at the EH for the 3 sites on which we concentrate here. For this, we performed

CPD
7, 1845–1886, 2011

$\delta^{18}O$, d-*excess* and ^{17}O-*excess* simulations for each of the site (Vostok, EDC and TD) taking into account their different moisture source with different RH and temperature. This second constraint was not used in previous studies because they concentrated only on one site.

Moisture source conditions for the drilling sites Vostok, EDC and TD have been determined from the Lagrangian moisture source diagnostic of Sodemann et al. (2008), applied for Antarctic ice cores as described in Stohl and Sodemann (2009). Moisture source regions and the respective sea surface temperatures are thereby determined quantitatively along backward trajectories calculated with the Lagrangian particle dispersion model FLEXPART (Stohl et al., 2005). An advantage of the FLEXPART model over usual trajectory calculations is that turbulent and convective motions of air parcels are represented by parametrisations. Moisture sources are then identified along the air parcel's trajectories from changes in specific humidity within the boundary layer, and weighted according to sequence as described in Sodemann et al. (2008). Here, moisture sources for the Vostok, EDC and TD ice core sites are based on 1-year calculations covering the year 2005 using the ERA-Interim data set. 30000 particles have been released in a domain covering 70–80° S, 100–165° E, with new particles being traced according to mass flux into the domain (domain-filling run). Since Central Antarctica is one of Earth's most arid regions, the moisture diagnostic reaches its range of applicability, in particular for winter conditions. For example, clear sky precipitation (diamond dust) is not taken into account in the underlying model simulations, which may be a seasonally relevant contributor to accumulation at Vostok and EDC.

The moisture sources identified for the three ice core drilling sites identified here span a shorter time interval, but offer higher resolution than the previous results by Sodemann and Stohl (2009). On the annual mean, moisture source longitude is similar for the Vostok and EDC sites (60° E), while TD has more easterly moisture sources (100° E). More importantly, the three drilling sites have different source latitudes, with Vostok having the most northerly location at 42° S, followed by EDC (44° S) and TD (46° S). As shown by Masson-Delmotte et al. (2011), seasonal variation of the moisture origin

CPD
7, 1845–1886, 2011

is largest between the time of maximum (August–September–October) and minimum (January–February–March) sea ice cover.

4 Results

4.1 Temporal distribution of ^{17}O – *excess* at Vostok, EPICA Dome C (EDC) and Talos Dome (TD)

Figures 2a to 2c display the record of ^{17}O-*excess* and δ^{18}O during the last deglaciation from Vostok, EDC and TD ice cores (δ^{18}O -references: Vimeux et al., 1999; EPICA-Members, 2004; and Stenni et al., 2001; Stenni et al., 2003). The ^{17}O-*excess* data from Vostok were obtained at the institute of Earth Sciences in Jerusalem and published in Landais et al. (2008). The ^{17}O-*excess* records for EDC and TD were obtained at LSCE. The thick lines represent a 5 point moving average. During the period from LGM to EH, ^{17}O-*excess* increases by about 20 ppm for the Vostok site. Our ^{17}O-*excess* results of EDC show an increase of 13 ppm. For TD we do not evidence any clear trend over the last deglaciation and ^{17}O-*excess* stays around a mean level of 5.3 ppm for the whole period.

4.2 Statistical analysis

At first sight, it is not evident to draw robust conclusions on the temporal evolution of ^{17}O-*excess* at EDC and TD, since the scattering of the data is quite large. We performed a statistical analysis of our data in order to check if the mean ^{17}O-*excess* levels for LGM and EH significantly differ. For simplicity, we mention in this chapter only the conclusions of this analysis, the detailed description being given in the Appendix A. First, we compared the ^{17}O-*excess* mean values of LGM and EH for the sites of EDC and TD. Significance was tested by computing the two-sample confidence bounds, which yielded a higher ^{17}O-*excess* mean level for EH compared to LGM for the site of

CPD
7, 1845–1886, 2011

EDC, but not for TD. Since this test contains only a limited number of data points (which correspond to the period of LGM and EH, respectively), it does not provide a tool to reproduce the trend of ^{17}O-*excess* during the complete period. So, in a second step we performed a regression analysis which includes all data points of the considered records at EDC and TD (58 data points for EDC and 44 for TD). Several fit functions with different degrees of freedom were tested (F-tests) and the most robust one was obtained when using a linear function. The result of the linear fit for the EDC-data was an increase of 13 ppm during the period from LGM to EH. In contrast, no significant temporal gradient of ^{17}O-*excess* was obtained for TD (Fig. 4a and b in Appendix A).

4.3 Results and limits of the MCIM

Table 1 displays the results of MCIM simulation for the three sites of our studies after adjustment of the tuning parameters to best fit the δ^{18}O , ^{17}O-*excess* and d-*excess* on the transect Terra Nova Bay – Dome C and the mean isotopic values of EH at Vostok, EDC and TD.

We can make the following statements:

1. The δ^{18}O data are well reproduced by the MCIM for EDC and TD. The difference between data and modelled δ^{18}O for Vostok is with 3 ‰ higher than the differences at EDC and TD, respectively.

2. The modelled d-*excess* corresponds rather well to the data and the relative variation for the sites of Vostok and EDC. However d-*excess* is 5.6 ‰ too low for TD.

3. The MCIM reproduces well the ^{17}O-*excess* level at Vostok as well as the relative variation between EDC and TD. But the modelled ^{17}O-*excess* is 20 to 30 ppm too high for EDC and TD, compared to the data.

4. Modification of the supersaturation function S can improve the agreement between e.g. modelled and measured d-*excess* at TD or modelled and measured relative ^{17}O-*excess* variation between Vostok and EDC. However in this case, the

CPD
7, 1845–1886, 2011

modelled d-*excess* and ^{17}O-*excess* levels and relative variations are no more in agreement with the isotopic data measured on the Antarctic transect nor with the ^{17}O-*excess* variations between EDC and TD.

Actually it is not surprising to obtain such a discrepancy between some observations and the MCIM outputs. Indeed, the MCIM (Ciais and Jouzel, 1994) has first been dedicated to interpret water isotopic profiles at Vostok, and previous studies (Masson-Delmotte et al., 2008), (Vimeux et al., 2001) always used different tunings for different sites. We thus expect that the MCIM, with one single tuning configuration, can not fit water isotopes all over Antarctica. Yet our goal was not to reproduce very precisely the absolute values of the data, but to better understand the influence of the climatic parameters (RH , T_{site} and T_{source}) on d-*excess* and ^{17}O-*excess* to interpret their changes over the deglaciation. Therefore, in a second step, we varied the different tuning parameters, in order to investigate quantitatively the change of sensitivity of the isotopic ratios to the climatic parameters (RH, T_{site} and T_{source}). We give some examples of these sensitivity studies below:

1. We increased the proportion of re-evaporation (γ) of the liquid phase in the cloud by a factor of 10. The dashed lines in Fig. 3 show that increasing γ by a factor of 10, decreases the level of ^{17}O-*excess* by 10 to 18 ppm, which brings in better agreement the data and model output. In tandem, the sensitivity of ^{17}O-*excess* to T_{source} and RH increased by almost 100 % and 20 %, respectively. This tuning parameter has a negligible influence on d-*excess*. Such a test is not necessarily very realistic, but confirms that while ^{17}O-*excess* in polar ice keeps the signature of ^{17}O-*excess* in the low latitudes region of evaporation, the ice d-*excess* signature mainly results from the fractionation along the distillation path.

2. We found that the sensitivity of ^{17}O-*excess* and d-*excess* to T_{site} depends almost entirely on the tuning of the supersaturation function S that we adjusted as for the transect study (Terra Nova Bay – EDC): $S = 1 - 0.0033\ T_c$. Figure 3 shows that the tuning of supersaturation with temperature (δ^{18}O) is more important for

CPD
7, 1845–1886, 2011

the remote sites of Vostok and EDC (δ^{18}O between −50 to −62 ‰), where supersaturation is expected to be higher. At Vostok and EDC, $\frac{\Delta^{17}O-excess}{\Delta T_{site}}$ can vary between −0.2 to 0.5 ppm °C $^{-1}$ for $S = 1 - 0.002\ T_c$ to $S = 1 - 0.004\ T_c$. At the coastal site of TD (δ^{18}O between −36 to −40.5 ‰), the co-variation of ^{17}O-*excess* with T_{site} remains within the 6 ppm (equally our measurement uncertainty) in the above relatively large range of supersaturation dependency. Such sensitivity of ^{17}O-*excess* to supersaturation tuning highlights the importance of mapping ^{17}O-*excess* spatial variations for different periods (LGM, EH, ...) to help constrain isotopic fractionation on snow formation.

3. We performed dozens of sensitivity studies varying the other tuning parameters (fraction of condensate remaining in the cloud, the temperature range where liquid and solid water can coexist and the parameter which controls at what temperature the first ice forms). We found that they do not change the sensitivity of d-*excess* and ^{17}O-*excess* to the climatic parameters (RH , T_{site} and T_{source}) significantly. Note also that wind speed has no significant impact on our findings.

We carried out no studies concerning the sensitivity of the d-*excess* and ^{17}O-*excess* to the fractionation factors $^{17}\alpha$, $^{18}\alpha$ and $^{2H}\alpha$. If we would have used the ratio of the diffusion constants (see Sect. 2.2), obtained by Cappa et al. (2003) instead of Merlivat (1978), it would mainly affect the sensitivity of d-*excess* to climatic conditions. Below we summarize the output of our sensitivity studies in a linear equation, which represents the span of the sensitivities of each climatic parameter. Only the supersaturation has been strongly tuned, as described above.

$$\Delta^{17}O - excess = -(0.86 \text{ to } 1.1)\Delta RH - (-0.2 \text{ to } 0.5)\Delta T_{site} + (0.34 \text{ to } 0.61)\Delta T_{source} \quad (8)$$

$$\Delta d - excess = -(0.045 \text{ to } 0.095)\Delta RH - (1.29 \text{ to } 2.04)\Delta T_{site} + (1.31 \text{ to } 1.5)\Delta T_{source}$$

$$-3\Delta\delta^{18}O_{ocean}$$

CPD
7, 1845–1886, 2011

The dependency of Δd-*excess* on the isotopic composition of the ocean ($\delta^{18}O_{ocean}$) has been obtained as depicted in Jouzel et al. (2003). This coefficient depends only on the isotopic composition ($\delta^{18}O$ and $\delta^{2}H$) of the polar site of interest. Its absolute value increases with decreasing $\delta^{2}H$ or $\delta^{18}O$. $\Delta\delta^{18}O_{ocean}$ does not change ^{17}O-*excess* , due to its logarithmic definition (Landais et al., 2009).

The coefficients obtained in Eq. (8) are rather close to what was obtained previously by Landais et al. (2009) or Risi et al. (2010) for the Vostok site. ^{17}O-*excess* mainly depends on OSR RH; the relatively high sensitivity of ^{17}O-*excess* with T_{source} is only obtained in an unrealistic case of very high re-evaporation of the liquid phase in the cloud. The modelled variations of d-*excess* with climatic conditions at the source are also comparable with the previous studies of Vimeux et al. (2001) and Stenni et al. (2001). However, as already discussed in Landais et al. (2009) and Risi et al. (2010), the sensitivity of d-*excess* with T_{site} increases especially on the central sites because of the tuning of the supersaturation imposed by the stability of ^{17}O-*excess* in Antarctica.

5 Discussion

1. From the comparison of the three Antarctic ^{17}O-*excess* profiles, we conclude that the Antarctic ^{17}O-*excess* evolution over the deglaciation displays strong regional differences. In particular, the strong increase at Vostok is not observed with the same magnitude at the site of EDC and no shift is detected at the coastal site of TD. The first conclusion from this study is that the ^{17}O-*excess* signal that was recorded at Vostok (Landais et al., 2008) is a signal with regional peculiarities that can not be generalized to all Antarctica.

2. Second, from the three sites presented here, we note a clear modern spatial gradient of the ^{17}O-*excess* mean level at EH from the more coastal site (TD, 2.6 ppm) to the most remote one (Vostok, 40 ppm), EDC being associated with an intermediate ^{17}O-*excess* level (23 ppm). This evolution from the coast to the

CPD
7, 1845–1886, 2011

East Antarctic plateau is different from the ^{17}O-*excess* evolution measured over a transect on the same region of Antarctica (Landais et al., 2008) that does not exhibit any clear trend from the coast to central East Antarctica.

3. We propose an explanation for the different mean levels of ^{17}O-*excess* at EH and for the different trends over the deglaciation for the 3 sites based on the MCIM detailed above. From the MCIM outputs (Eqs. 8), we can exclude different T_{source} as an explanation for different ^{17}O-*excess* mean levels and trends. In contrast, source RH can have a strong influence. The large difference in ^{17}O-*excess* between the continental sites of Vostok and EDC compared to the coastal one at TD can be explained by different OSRs (with different RH) for the two regions as indicated by the results of the back trajectory model (Sect. 3.2.1). For Vostok and EDC, the model diagnosed moisture sources over the interior of Antarctica. These continental moisture sources are probably due to evaporation/sublimation of surface snow and may increase ^{17}O-*excess* at Vostok and EDC. TD has a completely different pattern of moisture sources, where all the moisture stems from OSRs (Fig. 5a, b and c in the Appendix B). The difference of 20 ppm between ^{17}O-*excess* mean levels at Vostok and EDC is more compelling. The sparsity of precipitation events makes it difficult to distinguish the moisture origin of Vostok from the one of EDC. However, higher d-*excess* and ^{17}O-*excess* at Vostok may be due to different OSRs and moisture trajectories. The latter may also result in water vapour recycling, which causes unequal imprints in ^{17}O-*excess* for Vostok and EDC, respectively. Indeed, Ekaykin et al. (2004) suggested that Vostok is influenced by moisture stemming from the Pacific coast, whereas the moisture of EDC is mainly (85 %) coming from the western Indian ocean (Scarchilli et al., 2010; Sodemann and Stohl, 2009; Werner et al., 2001).

4. Different seasonality of precipitation at Vostok and EDC may change mean level and evolution of ^{17}O-*excess* during the deglaciation. Indeed, Risi et al. (2010) showed that a change in the seasonality can have a significant influence on

CPD
7, 1845–1886, 2011

^{17}O-*excess* because of a mixing effect. Today, for both sites, the precipitation occurs all year round (Gallee and Gorodetskaya, 2010; Ekaykin et al., 2004) and the back trajectory analysis revealed similar seasonality for both sites. Another possibility, based on the MCIM, to explain the different ^{17}O-*excess* levels, is to invoke a strong change in the supersaturation dependency on temperature between Vostok and EDC. We have indeed mentioned in the last section that ^{17}O-*excess* mean level and the dependency on local temperature are very sensitive to the tuning of the supersaturation through kinetic fractionation. To explain a difference of 20 ppm between ^{17}O-*excess* at Vostok and EDC, the supersaturation dependency on temperature should be smaller than the one used in Eq. (8): $S = 1 - 0.001\ T_c$ instead of $1 - 0.0033\ T_c$. This explanation is rather tempting, since it also better explains, regarding the given tuning of the MCIM, the difference in d-*excess* observed between Vostok and EDC: it predicts a change of d-*excess* by 3.3 ‰ (instead of 2 ‰ which are given in Table 1) and is therefore in better agreement with the measured difference of 5.7 ‰.

5. Furthermore Vostok may be affected by local ^{17}O-*excess* inputs such clear sky precipitation (diamond dust) or stratospheric water vapour inputs (Stohl and Sodemann, 2009; Miller, 2008; Zahn et al., 1998). Franz and Röckmann (2005) reported a ^{17}O-anomaly of 0 ± 1800 ppm in lowermost stratospheric water vapour over Antarctica. Due to the large uncertainty of this result, the ^{17}O-anomaly of water vapour from the stratosphere may be greater than zero and therefore may influence ^{17}O-*excess* of precipitation at Vostok significantly.

6. The stability of ^{17}O-*excess* observed at TD over the deglaciation is in agreement with the interpretation given by the MCIM. δ^{18}O increases from −40.5 to −36.5 ‰ and within this range ^{17}O-*excess* does not depend on the choice of the supersaturation function (Fig. 3). The back trajectory model depicted no seasonality in the precipitation pattern for TD and it is difficult to imagine that the situation was different for EH (Laepple et al., 2011). Following the interpretation of the MCIM,

CPD
7, 1845–1886, 2011

decreasing ^{17}O-*excess* at TD would be attributed to an increase in RH at the OSR. The low ^{17}O-*excess* at TD thus reflects high latitudes OSR in the Austral Ocean, a finding which is supported by the back trajectory model. High latitude OSR, near the Antarctic coast, are marked by high RH (≈90 % for present-day, source: NCEP http://www.esrl.noaa.gov/), and therefore we do not expect decreasing RH at the OSR of TD during the deglaciation. Furthermore, Risi et al. (2010) found, based on model outputs from PMIP2 (http://pmip2.lsce.ipsl.fr/), nearly unchanged distribution of RH in the Austral ocean between LGM and EH. Still, we did not explore the possible influence on RH due to a shift of the sea ice margins. For the ^{17}O-*excess* increase over the deglaciation at EDC, the MCIM would suggest a decrease of the source RH by 10 %, with $S = 1 - 0.0033\ T_c$ ($S = 1 - 0.001\ T_c$ would require a 20% decrease of RH which is far too important). The OSR for EDC is situated at lower latitudes than the OSR for TD and an unequal variation of RH for two different OSRs in the Austral ocean during the deglaciation can not be excluded. A shift in RH of 10 % does not necessarily mean that the same OSR underwent such a change, since moisture origin of one site may be geographically different for EH and LGM, respectively. An increasing number of studies (Mc Glone et al., 2010; Lamy et al., 2010; Putnam et al., 2010) suggest major shifts in intensity and location of the southern westerlies during the last deglaciation. These changes may have modified the climatic conditions at the ocean surface as well as the location of the more important evaporation zones. Such effect could also explain the rapid d-*excess* shift, observed at EDC, at the end of Termination 2 (Masson-Delmotte et al., 2010) and has probably also an influence on ^{17}O-*excess* . The lack of present-day equivalent for LGM conditions at Vostok, EDC and TD remains a limitation for solid interpretation of isotopic signals in these regions.

CPD
7, 1845–1886, 2011

6 Summary and conclusion

We obtained ^{17}O-*excess* records spanning the last deglaciation for the sites of Dome C (EDC) and of Talos Dome (TD) (East Antarctica) and compared these results with the first profile previously obtained from the Vostok ice core (Landais et al., 2008). The data depict two important results:

1. EH mean levels of ^{17}O-*excess* are different for all three Antarctic ice core sites.
2. The three sites are marked by different evolution of ^{17}O-*excess* during the last deglaciation.

At EDC, which is marked by continental climatic conditions, we observed an increasing trend in ^{17}O-*excess* , from 10 (LGM) to 23 (EH) ppm, hence smaller than the 20 ppm (LGM = 20 ppm, EH = 40 ppm) rise at Vostok. At TD, which is a coastal site, a stable ^{17}O-*excess* of 5 ppm was measured throughout the last deglaciation.
The different levels of ^{17}O-*excess* between Vostok, EDC and TD at EH are consistent with unequal modern RH of the OSR as expected from our current understanding of ^{17}O-*excess* in polar regions. The lower ^{17}O-*excess* for TD, compared to the one at EDC, reflects the influence of OSR from higher latitudes and therefore higher RH (Scarchilli et al., 2010; Sodemann and Stohl, 2009).
We explain the unequal evolution of ^{17}O-*excess* for Vostok, EDC and TD respectively, with a different glacial/interglacial change in RH at their respective OSRs. Following this interpretation, RH of the OSR for TD remained almost constant, where as RH of the OSR for EDC changed by 10 %. A change in humidity conditions of the OSR for EDC may be linked to the modifications of strength and location of the westerlies (Mc Glone et al., 2010; Lamy et al., 2010). From the MCIM (tuned for the transect study from Terra-Nova Bay to EDC) results, we conclude that ^{17}O-*excess* can serve as marker of RH of the OSR in the coastal region of Antarctica. For the remote continental sites of East Antarctica we found that the dependence of ^{17}O-*excess* on local temperature is highly sensitive to the choice of the supersaturation function S. Such effect is also true

CPD
7, 1845–1886, 2011

for d-*excess*. It follows that local effects may significantly contribute to the ^{17}O-*excess* and d-*excess* signals at Vostok and to a lesser degree at EDC.

Finally, our work has two important consequences. First, it demonstrates that the previous ^{17}O-*excess* profile measured at Vostok (during the last deglaciation) is a regional signal and should therefore not be interpreted as a decrease in RH of the Southern ocean as it has been suggested in Landais et al. (2008); local effects such as changes in supersaturation or stratospheric inputs may be at play. Therefore reconstructing past RH of the OSR is more reliable from coastal ice cores. Second, the particular sensitivity of ^{17}O-*excess* to supersaturation should not be seen as a disadvantage for paleo climatic reconstruction: ^{17}O-*excess* spatial distributions for different periods could help to constrain the supersaturation dependency to temperature and thus help to interpret climatic signals of δ^{18}O and d-*excess*.

7 Outlook

^{17}O-*excess* measurements on other sites, such as EPICA Dronning Maud Land, Law Dome and Berkner will expand the spatial distribution of ^{17}O-*excess* records in Antarctica and therefore could give constraints on the accurate tuning of the supersaturation function in the MCIM. The analysis of surface snow and of snowpits from Vostok will let us depict seasonal and inter annual variations of ^{17}O-*excess*. The comparison of ^{17}O-*excess* data, stemming from the Vostok site, with ice core proxies for stratospheric inputs (tritium, Be10) will help to quantify the influence of non-mass-dependent fractionation effects on ^{17}O-*excess*. Isotopic analysis of surface snow and at the same time of the water vapour of the lowest atmosphere layer in polar regions should allow us to get information about post-deposit isotopic fractionation processes, such as local recycling due to evaporation/sublimation.

CPD
7, 1845–1886, 2011

Appendix A

Statistics

A1 Two sample confidence bounds

In order to compare the two mean levels μ_E and μ_L of ^{17}O-*excess* for EH and LGM, respectively, we computed a two sample confidence interval for their difference $\mu_E - \mu_L$, for the data of EDC and TD separately. For both ice core sites, we took samples of data points corresponding to the same period: The epoch of EH spans the period from 9 to 12 ka with data points $E_1, E_2, \ldots, E_n$, the epoch of LGM contains the period from 20 to 25 ka with data points $L_1, L_2, \ldots, L_m$. We estimated the unknown mean values μ_E and μ_L by the sample means $\bar{E} = n^{-1} \sum_{i=1}^{n} E_i$ and $\bar{L} = m^{-1} \sum_{i=1}^{m} L_i$, respectively. With S_E and S_L denoting the corresponding sample standard deviations, one can compute the following two-sample confidence bounds for $\mu_E - \mu_L$:

$$\bar{E} - \bar{L} \pm \sqrt{\frac{n+m}{n\,m}}\, S\, t_{n+m-2;0.975} \tag{A1}$$

$$S = \sqrt{\frac{(n-1)S_E + (m-1)S_L}{n+m-2}} \tag{A2}$$

where S corresponds to the estimated standard deviation of a single measurement, and $t_{n+m-2;0.975}$ denotes the 97.5 %-quantile of student's t-distribution e.g. (Papula, 2001) with $m+n-2$ degrees of freedom. With 95 % confidence we may conclude that the unknown difference $\mu_E - \mu_L$ is between these two confidence bounds. Using Eq. (A1), we end up with the confidence bounds 7.01 and 15.13 for EDC, so there is evidence that $\mu_E - \mu_L$ is strictly greater than zero. For TD, the confidence bounds are −10.04 and 5.19, so there is no evidence for $\mu_E - \mu_L$ being different from zero. In other words, the computation of the two-sample confidence bounds evidenced a significant

CPD
7, 1845–1886, 2011

increase in ^{17}O-*excess* at EDC during the last deglaciation. For TD, the observed difference $\bar{E} - \bar{L}$ was not significantly different from zero. Table 2 summarizes these results for EDC and TD.

A2 Regression analysis

To obtain a statistical tool to depict a possible trend in ^{17}O-*excess* at EDC and perhaps as well at TD we performed a regression analysis, using the open source software *R* (R Development Core Team, 2011).

Generally we assume that the i-th measurement equals $Y_i = f(X_i) + \epsilon_i$ for an unknown regression function f and measurement errors ϵ_i, where X_i corresponds to the age in ka while i runs from 1 to 58 for EDC and from 1 to 44 for TD. Assuming a certain type of f, we estimated it via least squares as $\hat{f}$, and this fitted function yielded the residuals $\hat{\epsilon}_i = Y_i - \hat{f}(X_i)$. Scatter plots of the pairs $(\hat{\epsilon}_i, \hat{\epsilon}_{i+1})$ showed no correlation, so we assumed the errors ϵ_i to be independent. Moreover, a normal QQ-plot of the residuals supported the assumption of the errors being Gaussian, so we applied standard methodology for regression models.

First we assumed a linear trend in ^{17}O-*excess* for the considered period of the last deglaciation. That means, we considered the family of all linear functions, $f_{\text{lin}}(x) = a + b\,x$, to explain our data of ^{17}O-*excess* , where a is the ordinate intercept (= ^{17}O-*excess* at present), b the gradient of ^{17}O-*excess* during the period from LGM to EH and x is the age in ka. In order to check if nonlinear functions with more degrees of freedom would fit our data more accurately, we performed F-tests of a linear trend versus the alternative hypothesis of a (i) quadratic function f, (ii) a cubic function f and (iii) a cubic spline f with four knots. The high p-values of these F-tests (p(i) = 0.35, p(ii) = 0.51 and p(iii) = 0.84) indicate that there is no evidence for a nonlinear trend of ^{17}O-*excess* at EDC. The same conclusion is true for the regression analysis of ^{17}O-*excess* at TD, where we obtained the following p-values of the F-tests: p(i) = 0.61, p(ii) = 0.72 and p(iii) = 0.44.

CPD
7, 1845–1886, 2011

Table 3 displays the result of the linear regression analysis. There the p-value is for the null hypotheses of no trend at all, i.e. a constant level of ^{17}O-*excess* and $b = 0$. The very low p-value at EDC indicates that there is a significant linear increase of 13 ppm ($\hat{f}_{\mathrm{lin}}(\mathrm{EH}) - \hat{f}_{\mathrm{lin}}(\mathrm{LGM}) = 0.72(-7 + 25) = 12.96$) during the last deglaciation. For TD, the regression analysis yield no significant temporal gradient during the period from 25 to 8 ka.

Appendix B

Lagrangian moisture source diagnostics

Figures 5, b and c show the moisture sources (as fractions) identified from the Lagrangian diagnostics of Sodemann et al. (2008) using a 1-year simulation (October 2004–November 2005, ECMWF analysis data) of FLEXPART run in domain-filling backward mode over a sector of East Antarctica. The extraction threshold was fixed at 0.005 g/kg/3h.

The seasonality of Vostok and EDC are similar, but different enough to be distinguished, in particular during MAM. For Vostok, particularly during DJF, moisture sources are diagnosed over the interior of Antarctica, indicating either evaporation/sublimation during the summer or (less likely, but not to be excluded) artifacts e.g. from data analysis. However, the same inland sources also show up for EDC. Coastal moisture sources show up as well, possibly indicating moistening of higher altitudes due to boundary-layer venting at the orography or land-sea transition. TD has a completely different pattern of moisture sources, being a more low-altitude coastal site: compared to Vostok and EDC high latitudinal OSRs are more important and there are no sources from the interior of the Antarctic continent diagnosed.

Acknowledgements. This work is a contribution to the European Project for Ice Coring in Antarctica (EPICA), a joint European Science Foundation/European Commission scientific programme, funded by the EU (EPICA-MIS) and by national contributions from Belgium, Denmark,

CPD
7, 1845–1886, 2011

France, Germany, Italy, the Netherlands, Norway, Sweden, Switzerland and the United Kingdom. The Talos Dome Ice core Project (TALDICE), a joint European programme, is funded by national contributions from Italy, France, Germany, Switzerland and the United Kingdom. The work (fluorination, IRMS) done at LSCE, is funded by the ANR CITRONNIER. We thank Franoise Vimeux for providing samples from the Vostok ice core and Ryu Uemura for the fruitful discussions and for the cross-read of the manuscript. Thanks also go to the Marie Curie Initial Training Network INTRAMIF (FP7), which has funded R. Winkler's PhD at LSCE-IPSL-CEA.

The publication of this article is financed by CNRS-INSU.

References

Angert, A., Cappa, C. D., and Paolo, D. D.: Kinetic $\delta^{17}O$ effects in the hydrological cycle: Indirect evidence and implications, Geochim. Cosmochim. Acta, 68, 3487–3495, 2004. 1847

Barkan, E. and Luz, B.: High precision measurements of $^{17}O/^{16}O$ and $^{18}O/^{16}O$ ratios in H_2O, Rapid Communciation in Mass Spectrometry, 19, 3737–3742, 2005. 1847, 1849, 1851, 1852

Barkan, E. and Luz, B.: Diffusivity fractionations of $H_2^{16}O/H_2^{17}O$ and $H_2^{16}O/H_2^{18}O$ in air and their implications for isotope hydrology, Rapid Communciation in Mass Spectrometry, 21, 2999–3005, 2007. 1850, 1851

Cappa, C., Hendricks, M. B., De Paolo, D. J., and Cohen, R.: Isotopic fractionation of water during evaporation, J. Geophys. Res., 108, 4525–4535, 2003. 1849, 1860

Ciais, P. and Jouzel, J.: Deuterium and oxygen 18 in precipitation: Isotopic model, including mixed cloud processes, J. Geophys. Res., 99, 16793–16803, 1994. 1847, 1848, 1853, 1854, 1855, 1859

CPD
7, 1845–1886, 2011

Craig, H.: Isotopic standards for carbon and oxygen and correction factors for mass spectrometric analysis of carbon dioxide., Geochim. Cosmochim. Acta, 12, 133–149, 1957. 1850
Craig, H.: Isotopic Variations in Meteoric Waters, Science, 133, 1702–1703, 1961. 1851
Craig, H. and Gordon, L.: Deuterium and oxygen 18 variations in the ocean and the marine atmosphere., Symposium on Marine Geochemistry, Narraganset Marine Laboratory, University of Rhode Island Publication, 3, 277–374, 1965. 1847
Dansgaard, W.: Stable isotopes in precipitation, Tellus, 169, 436–468, 1964. 1847, 1851
Delmotte, M., Masson, V., Jouzel, J., and Magon, V.: A seasonal deuterium excess signal at Law Dome, coastal Eastern Antarctica: A Southern ocean signature, J. Geophys. Res., 105, 7187–7197, 2000. 1854
Ekaykin, A. and Lipenkov, V. Y.: Formation of the Ice Core Isotopic Composition, in: *PICR II"Physics of Ice-Core Records"*, edited by: Hondoh, T., Institue of Low Temperature Science, Hokkaido University Press, Sapporo, 299–314, 2009. 1855
Ekaykin, A. A., Lipenkov, V. Y., Kuzmina, I., Petit, J.-R., Masson-Delmotte, V., and Johnsen, S. J.: The changes in isotope composition and accumulation of snow at Vostok station, East Antarctica, over the past 200 years, Ann. Glaciol., 39, 569–575, 2004. 1862, 1863
EPICA-Members: Eight glacial cycles from Antarctic ice core, Nature, 429, 623–628, 2004. 1857
Franz, P. and Röckmann, T.: High-precision isotope measurements of $H_2^{16}O$, $H_2^{17}O$ and $H_2^{18}O$ and the $\Delta^{17}O$-anomaly of water vapour in the Southern lowermost stratosphere, 2005. 1863
Gallee, H. and Gorodetskaya, I.: Validation of a limited area model over Dome C, Antarctic Plateau, during winter, Clim. Dynam., 34, 61–72, 2010. 1863
Gat, J. R. and Mook, W. G.: Stable Isotope processes in the water cycle, Environmental Isotopes in the Hydrological cycle, edited by W. G. Mook. chap. 3. U. N. Educ. Sci. and Cult. Org. IAEA, Paris, 2, 17–42, 1994. 1851
Johnsen, S., Dansgaard, W., and White, J.: The origin of Arctic precipitation under present and glacial conditions, Tellus, 41, 452–468, 1989. 1853
Jouzel, J. and Koster, R. D.: A reconsideration of the initial conditions used for stable water isotope models, J. Geophys. Res., 101, 22933–22938, 1996. 1854
Jouzel, J. and Merlivat, L.: Deuterium and Oxygen 18 in precipitation: Modelling of the isotopic effects during snow formation, J. Geophys. Res., 89, 11749–11757, 1984. 1854, 1855
Jouzel, J., Merlivat, L., and Lorius, C.: Deuterium excess in an East Antarctic ice core suggests higher relative humidity at the oceanic surface during the last glacial maximum, Nature, 299,

CPD
7, 1845–1886, 2011

688–691, 1982. 1847
Jouzel, J., Vimeux, F., Caillon, N., Delaygue, G., Hoffmann, G., Masson-Delmotte, V., and Parrenin, F.: Magnitude of isotope/temperature scaling for interpretation of Central Antarctic ice cores, J. Geophys. Res., 108, 4361–4372, 2003. 1861
Jouzel, J., Masson-Delmotte, V., Cattani, O., Dreyfus, G., Falourd, S., Hoffmann, G., Minster, B., Nouet, J., Barnola, J., Chapellaz, J., Fischer, H., Gallet, J., Johnsen, S., Leuenberger, M., Loulergue, L., Lthi, D., Oerter, H., Parrenin, F., Raisbeck, G., Raynaud, D., Schilt, A., Schwander, J., Selmo, E., Souchez, R., Spahni, R., Stauffer, B., Steffensen, J., Stenni, B., Stocker, T., Tison, J., Werner, M., and Wolff, E.: Orbital and Millenial Antarctic Climate Variability over the Past 800'000 Years, Science, 2007. 1846
Kaiser, J.: Consistent calculation of aquatic gross production from oxygen triple isotope measurements, Biogeosciences Discuss., 8, 4015–4062, doi:10.5194/bgd-8-4015-2011, 2011. 1847
Kavanaugh, J. and Cuffey, K.: Space and time variation of δ^{18}O and dD in Antarctic precipitation revisited, Global Biogeochem. Cy., 17, 1017–1030, 2003. 1853
Laepple, T., Werner, M., and Lohmann, G.: Synchronicity of Antarcitc temperatures and local solar insolation on orbital timescales, Nature, 471, 91–94, 2011. 1863
Lamy, F., Kilian, R., Arz, H. W., François, J.-P., Kaiser, J., Prange, M., and Steinke, T.: Holocene changes in the position and intensity of the Southern westerly wind belt, Nat.Geosci., 3, 695–699, 2010. 1864, 1865
Landais, A., Barkan, E., and Luz, B.: Record of δ^{18}O and ^{17}O-excess in ice from Vostok Antarctica during the last 150'000 years, Geophys. Res. Lett., 35, L02709–L02713, 2008. 1846, 1847, 1848, 1853, 1854, 1855, 1857, 1861, 1862, 1865, 1866
Landais, A., Barkan, E., Vimeux, F., Masson-Delmotte, V., and Luz, B.: Combined Analysis of Water Stable Isotope ($H_2^{16}O$, $H_2^{17}O$, $H_2^{18}O$, $HD^{16}O$), in: *PICR II"Physics of Ice-Core Records"*, edited by: Hondoh, T., Institue of Low Temperature Science, Hokkaido University Press, Sapporo, 315–327, 2009. 1861
Luz, B. and Barkan, E.: The isotopic ratios $^{17}O/^{16}O$ and $^{18}O/^{16}O$ in molecular oxygen and their significance in bio-geochemistry, Geochim. Cosmochim. Acta., 69, 1099–1110, 2004. 1850
Luz, B. and Barkan, E.: Net and gross oxygen production from O-2/Ar, O-17/O-16 and O-18/O-16 ratios, Aquat. Microb. Ecol., 56, 133–145, 2009. 1853
Luz, B., Barkan, E., Bender, M. L., Thiemens, M. H., and Boering, K. A.: Triple-isotope composition of atmospheric oxygen as a tracer of biosphere productivity, Nature, 400, 547–550,

CPD
7, 1845–1886, 2011

1999. 1847
Luz, B., Barkan, E., Yam, R., and Shemesh, A.: Fractionation of oxygen and hydrogen isotopes in evaporating water, Geochim. Cosmochim. Acta., 73, 6697–6703, 2009. 1850
Majoube, M.: Fractionnement en ^{18}O entre la glace et la vapeur d'eau, J. Climate Phys., 1971a. 1849
Majoube, M.: Fractionnement en ^{18}O entre l'eau et sa vapeur d'eau, Journal Chem. Phys., 1971b. 1849
Masson-Delmotte, V., Stenni, B., and Jouzel, J.: Common millennial-scale variability of Antarctic and Southern Ocean temperatures during the past 5000 years reconstructed from the EPICA Dome C ice core, Holocene, 14, 145–151, 2004. 1854
Masson-Delmotte, V., Landais, A., Stievenard, M., , Cattani, O., Falourd, S., Jouzel, J., Johnsen, S., Dahl-Jensen, D., Sveinsbjomdottir, A., White, J., and Popp, T.: Holocene climatic changes in Greenland: Different deuterium-excess signals at Greenland ice core project (GRIP) and NorthGRIP, J. Geophys. Res., 110, D14102–D14116, 2005. 1855
Masson-Delmotte, V., Hou, S., Ekaykin, A., Jouzel, J., Aristarain, A., Bernardo, R., Bromwich, D., Cattani, O., Delmotte, M., Falourd, S., Frezzotti, M., Gallée, H., Genoni, L., Isaksson, E., Landais, A., Helsen, M., Hoffmann, G., Lopez, J., Morgan, V., Motoyama, H., Noone, D., Oerter, H., Petit, J., Royer, A., Uemura, R., Schmidt, G., Schlosser, E., Simoes, J., Steig, E., Stenni, B., Stievenard, M., Van Den Broeke, M., Van de Waal, R., Van de Berg, W., Vimeux, F., and White, J.: A review of Antarctic surface snow isotopic composition: Observations, atmospheric circulation, and isotopic modeling, J. Climate, 21, 3359–3387, 2008. 1847, 1859
Masson-Delmotte, V., Stenni, B., Blunier, T., Cattani, O., Chapellaz, J., Cheng, H., Dreyfus, G., Edwards, R. L., Falourd, S., Govin, A., Kawamura, K., Johnsen, S., Jouzel, J., Landais, A., Lemieux-Doudon, B., Lourantou, A., Marshall, G., Minster, B., Mudelsee, M., Pol, K., Röthlisberger, R., Selmo, E., and Waelbroeck, C.: Abrupt change of Antarctic moisture origin at the end of Termination II, PNAS, 2010. 1864
Masson-Delmotte, V., Buiron, D., Ekaykin, A., Frezzotti, M., Gallée, H., Jouzel, J., Krinner, G., Landais, A., Motoyama, H., Oerter, H., Pol, K., Pollard, D., Ritz, C., Schlosser, E., Sime, L. C., Sodemann, H., Stenni, B., Uemura, R., and Vimeux, F.: A comparison of the present and last interglacial periods in six Antarctic ice cores, Clim. Past, 7, 397–423, doi:10.5194/cp-7-397-2011, 2011. 1848, 1856
Mc Glone, M., Turney, C. S. M., Wilmshurst, J. M., Renwick, J., and Pahnke, K.: Divergent

CPD
7, 1845–1886, 2011

trends in land and ocean temperature in the Southern Ocean over the past 18'000 years, Nature Geoscience, 3, 622–626, 2010. 1864, 1865

Meijer, H. A. J. and Li, W. J.: The use of electrolysis for accurate $\delta^{18}O$ and $\delta^{17}O$ Isotope measurements in water, Isotopes Environ. Health Stud., 34, 349–369, 1998. 1850

Merlivat, L.: The Dependence of Bulk Evaporation Coefficients on Air-Water Interfacial Conditions as Determined by the Isotopic Method, J. Geophys. Res., 83, 2977–2980, 1978. 1849, 1850, 1851, 1860

Merlivat, L. and Jouzel, J.: Global climatic interpretation of the deuterium-oxygen 18 relationship for precipitation, J. Geophys. Res., 84, 5029–5033, 1979. 1847, 1851, 1854

Merlivat, L. and Nief, G.: Fractionnement isotopique lors des changements d'Etat solid-vapeur et liquide-vapeur de l'eau des températures inférieures à 0 degrées C., Tellus, 1, 1967. 1849

Miller, M. F.: Isotopic fractionation and the quantification of ^{17}O anomalies in the oxygen three-isotope system: an appraisal and geochemical significance, Geochim. Cosmochim. Ac., 66, 1881–1889, 2002. 1850

Miller, M. F.: Comment on "Record of $\delta^{18}O$ and ^{17}O-excess in ice from Vostok Antarctica during the last 150'000 years" by Amaelle Landais et al., Geophys. Res. Lett., 35, L23709, 2008. 1863

Mook, W.: Environmental Isotopes in the Hydrological Cycle: Introduction, UNESCO IAEA, Paris, 1, 1994. 1849, 1851

Mook, W. G. and Grootes, P. M.: The measuring procedure and corrections for the high precision mass spectrometric analysis of isotopic abundance ratios, especially referring to carbon, oxygen and nitrogen, Int. J. Mass Spectrom. Ion Phys., 12, 273–298, 1973. 1850

Noone, D.: The influence of midlatitude and tropical overturning circulation on the isotopic composition of atmospheric water vapor and Antarctic precipitation, J. Geophys. Res., 113, D04102–D04114, 2008. 1853

Papula, L.: Mathematik für Ingenieure und Naturwissenschaftler Band 3, Viewegs Fachbücher der Technik, Braunschweig Wiesbaden, 740, 2001. 1867

Petit, J. R., White, J. W. C., Young, N. W., Jouzel, J., and Korotkevich, Y. S.: Deuterium Excess in recent Antarctic Snow, J. Geophys. Res., 96, 5113–5122, 1991. 1847, 1855

Putnam, A. E., Denton, G. H., Schaefer, J. M., Barrell, D. J. A., Andersen, B. G., Finkel, R. C., Schwartz, R., Doughty, A. M., Kaplan, M. R., and Schlüchter, C.: Glacier advance in Southern middle-latitudes during the Antarctic Cold Reversal, Nat. Geosci., 3, 700–704, 2010. 1864

CPD
7, 1845–1886, 2011

R Development Core Team: R: A Language and Environment for Statistical Computing, R Foundation for Statistical Computing, Vienna, Austria, http://www.R-project.org, ISBN 3-900051-07-0, 2011. 1868

Risi, C., Landais, A., Bony, S., Jouzel, J., Masson-Delmotte, V., and Vimeux, F.: Understanding the ^{17}O-*excess* glacial-interglacial variations in Vostok precipitation, J. Geophys. Res., 115, D10112–D10126, 2010. 1848, 1854, 1861, 1862, 1864

Scarchilli, C., Frezzotti, M., and Ruti, P.: Snow precipitation at four ice core sites in East Antarctica: provenance, seasonality and blocking factors, Clim. Dynam., 4, 0946–0964, 2010. 1862, 1865

Sodemann, H. and Stohl, A.: Asymmetries in the moisture origin of Antarctic precipitation, Geophys. Res. Lett., 36, L22803–L22807, 2009. 1856, 1862, 1865

Sodemann, H., Schwierz, C., and Wernli, H.: Interannual variability of Greenland winter precipitation sources: Lagrangian moisture diagnostic and North Atlantic Oscillation influence, Geophys. Res. Lett., 113, D03107–D03123, 2008. 1856, 1869

Stenni, B., Masson-Delmotte, V., Johnsen, S., Jouzel, J., Longinelli, A., Monnin, E., Röthlisberger, R., and Selmo, E.: An Oceanic Cold Reversal during the last deglaciation, Science, 293, 2074–2077, 2001. 1847, 1854, 1855, 1857, 1861

Stenni, B., Jouzel, J., Masson-Delmotte, V., Röthlisberger, R., Castellano, E., Cattani, O., Falourd, S., Johnsen, S. J., Longinelli, A., Sachs, J. P., Selmo, E., Souchez, R., Steffensen, J. P., and Udisti, R.: A late-glacial high-resolution site and source temperature record derived from the EPICA Dome C isotope records (East Antarctica), Earth Planet. Sci. Lett., 217, 183–195, 2003. 1855, 1857

Stenni, B., Masson-Delmotte, V., Selmo, E., Oerter, H., Meyer, H., Röthlisberger, R., Jouzel, J., Cattani, O., Falourd, S., Fischer, H., Hoffmann, G., Iacumin, P., Johnsen, S. J., Minster, B., and Udisti, R.: The deuterium excess records of EPICA Dome C and Dronning Maud Land ice cores (East Antarctica), Quarternary Sci. Rev., 29, 146–159, 2010. 1854, 1855

Stenni, B., Buiron, D., Frezzotti, M., Albani, S., Barbante, C., Bard, E., Barnola, J., Baroni, M., Baumgartner, M., Bonazza, M., Capron, E., Castellano, E., Chapellaz, J., Delmonte, B., Falourd, S., Genoni, L., Iacumin, P., Jouzel, J., Kipfstuhl, S., Landais, A., Lemieux-Dudon, B., Maggi, V., Masson-Delmotte, V., Mazzola, C., Minster, B., Montagnat, M., Mulvaney, R., Narcisi, B., Oerter, H., Parrenin, F., Petit, J., Ritz, C., Scarchilli, C., Schilt, A., Schübbach, S., Schwander, J., Selmo, E., Stocker, T., and Udisti, R.: Expression of the bipolar sea-saw in Antarctic climate records during the last deglaciation, Nat. Geosci., 4, 46–49, 2011. 1848

CPD
7, 1845–1886, 2011

Stohl, A. and Sodemann, H.: Characteristics of the atmospheric transport into the Antarctic troposphere, J. Geophys. Res., D02305–D02320, 2009. 1856, 1863

Stohl, A., Forster, C., Frank, A., Seibert, P., and Wotawa, G.: Technical note: The Lagrangian particle dispersion model FLEXPART version 6.2, Atmos. Chem. Phys., 5, 2461–2474, doi:10.5194/acp-5-2461-2005, 2005. 1856

Uemura, R., Barkan, E., Abe, O., and Luz, B.: Triple isotopic composition of oxygen in atmospheric water vapor, Geophys. Res. Lett., 37, L04402–L04405, 2010. 1847, 1851

Van Hook, W. A.: Vapour Pressures of Isotopic Waters and Ices, J. Phys. Chem.-US, 72, 1234–1244, 1968. 1849

Vimeux, F., Masson, V., Jouzel, J., Stievenard, M., and Petit, J. R.: Glacial-interglacial changes in the ocean surface conditions in the Southern Hemisphere, Nature, 398, 410–413, 1999. 1847, 1855, 1857

Vimeux, F., Masson, V., Delaygue, G., Jouzel, J., Petit, J. R., and Stievenard, M.: A 420,000 year deuterium excess record from East Antarctica: Information on past changes in the origin of precipitation at Vostok, J. Geophys. Res., 106, 31863–31873, 2001. 1854, 1855, 1859, 1861

Vimeux, F., Cuffey, K. M., and Jouzel, J.: New insights into Southern Hemisphere temperature changes from Vostok ice cores using deuterium excess correction, Earth Planet. Sci. Lett., 203, 829–843, 2002. 1847

Werner, M., Heimann, M., and Hoffmann, G.: Isotopic composition and origin of polar precipitation in present and glacial climate simulations, Tellus, 53, 53–71, 2001. 1862

Zahn, A., Barth, V., Pfeilsticker, K., and Platt, U.: Deuterium, Oxygen-18 and Tritium as tracers for water vapour transport in the lower stratosphere and tropopause region., Journal Atmos. Chem., 30, 25–47, 1998. 1863

CPD
7, 1845–1886, 2011

Table 1. Table 1 shows the output of the MCIM model, using the tuning that best fits the ^{17}O-*excess* $^{17}O-ex$ and d-*excess* data (d), obtained on the transect from Terra Nova Bay to EDC (Landais et al., 2008) and the isotopic values of EH at Vostok, EDC and TD. S ($= 1-0.0033\,T_c$) corresponds to the supersaturation function. OSRs were determined using the results of the back trajectory study (Sodemann et al., 2008 and Sodemann and Stohl, 2009). The model input T_{source} and RH for the three different sites were obtained by the use of NCEP-map http://www.esrl.noaa.gov/. The analytical error for the $\delta^{18}O$ measurements is 0.05 ‰ and 0.7 ‰ for d-*excess* (EPICA Members, 2004; Stenni et al., 2010, 2001 and Vimeux et al., 1999). The uncertainty for the ^{17}O-*excess* measurements is 6.4 ppm for EDC and 6.2 ppm for TD, respectively.

	Model						Measurements		
	T_{site} (°C)	T_{source} (°C)	RH	δ^{18}O (‰)	$^{17}O-ex$ (ppm)	d (‰)	δ^{18}O (‰)	$^{17}O-ex$ (ppm)	d (‰)
Vostok	−55.3	17	0.8	−53	50	15	−56	40	15
Dome C	−54.5	17	0.8	−51	50	13	−50.7	23	9.3
Talos Dome	−40.1	15	0.9	−38	38	−3	−36.6	2.6	2.6

CPD
7, 1845–1886, 2011

Table 2. This table shows the result of the performed two-sample confidence bounds: $\bar{E}$ and $\bar{L}$ are the estimated sample means of the data corresponding to EH and LGM, respectively. S_E and S_L denote the corresponding sample standard deviations and S corresponds to the estimated (common) standard deviation of the single measurements. n and m are the number of samples taken into account for the periods of EH and LGM, respectively. The last column corresponds to the upper and lower confidence bounds, respectively: with 95% confidence, $\mu_E - \mu_L$ lies between the lower and upper value.

	Two-sample confidence bounds						
	$\bar{E}$	$\bar{L}$	S_E	S_L	n	m	$\mu_E - \mu_L$
Dome C (EDC)	23	11.9	3.65	5.98	13	12	$7.01 \leq .. \leq 15.13$
Talos Dome (TD)	2.6	4.7	6.7	8.3	13	6	$-10.04 \leq .. \leq 5.19$

CPD
7, 1845–1886, 2011

Table 3. This table shows the result of the most robust regression function. The temporal gradient of ^{17}O-*excess* is reproduced by the linear functions with the ordinate intercept *a* and the gradient *b*. Explanation of significance level: very high (p-value < 0.001), high (p-value < 0.01), significant (p-value < 0.05), perhaps (p-value < 0.1), not significant (p-value > 0.1)

	Linear regression functions			
	a	*b*	p-value	significance level
Dome C (EDC)	27.3 ± 3.76	0.72 ± 0.24	0.005	high
Talos Dome (TD)	3.8 ± 1.4	−0.14 ± 0.07	0.797	not significant

CPD
7, 1845–1886, 2011

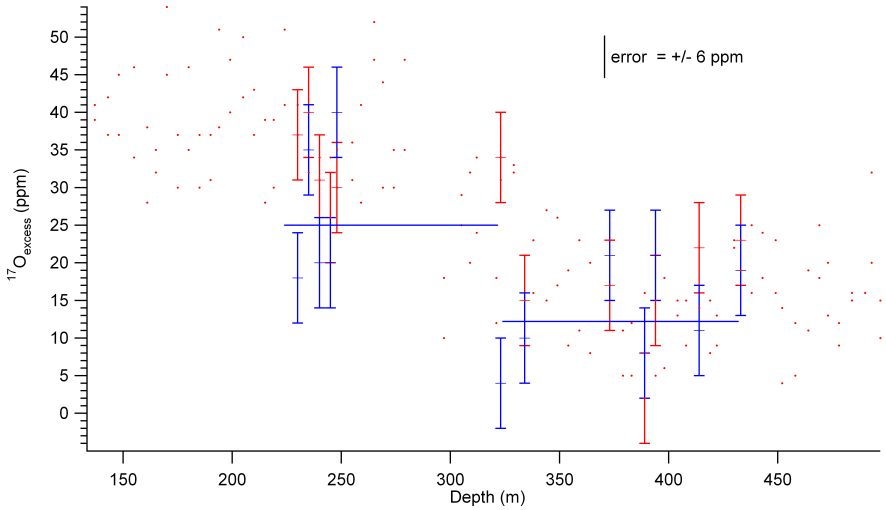

Fig. 1. Comparison of ^{17}O-*excess* measurements conducted at the Institute of Earth Science in Jerusalem and LSCE. We measured at LSCE (blue) ^{17}O-*excess* of 12 samples of the Vostok ice-core, previously measured by Landais et al. (2008) in Jerusalem (red). Apart two data points, the replica conducted at LSCE match (within the error of ±6 ppm) the previously obtained data. The blue lines represent the mean levels of the replica for EH (5 samples) and LGM (7 samples), respectively. We depicted a difference between the two mean levels of 13 ppm which corresponds very well to the increase (14 ppm for this data-subset) depicted by Landais et al. (2008).

CPD
7, 1845–1886, 2011

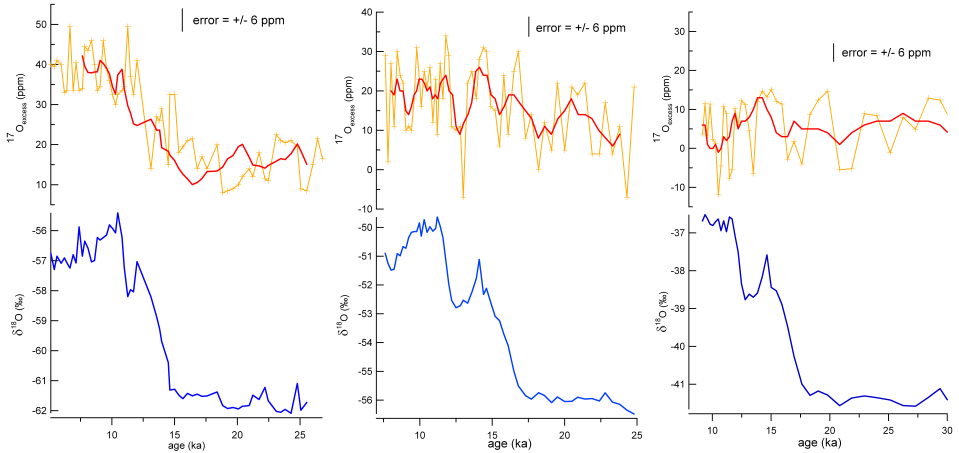

Fig. 2. Upper panel: record of ^{17}O-*excess* during the last deglaciation for the ice core sites of Vostok (**(a)**, from Landais et al., 2008), EDC **(b)** and TD **(c)**. The thick red lines represent a 5 point moving average. The temporal resolution of the data corresponds to about 2 data points per 1000 years. Lower panel (blue): δ^{18}O data previously published by: Vimeux et al. (1999) (Vostok), EPICA-Members, (2004), Stenni et al. (2001) (EDC) and Stenni et al. (2011), (TD).

CPD
7, 1845–1886, 2011

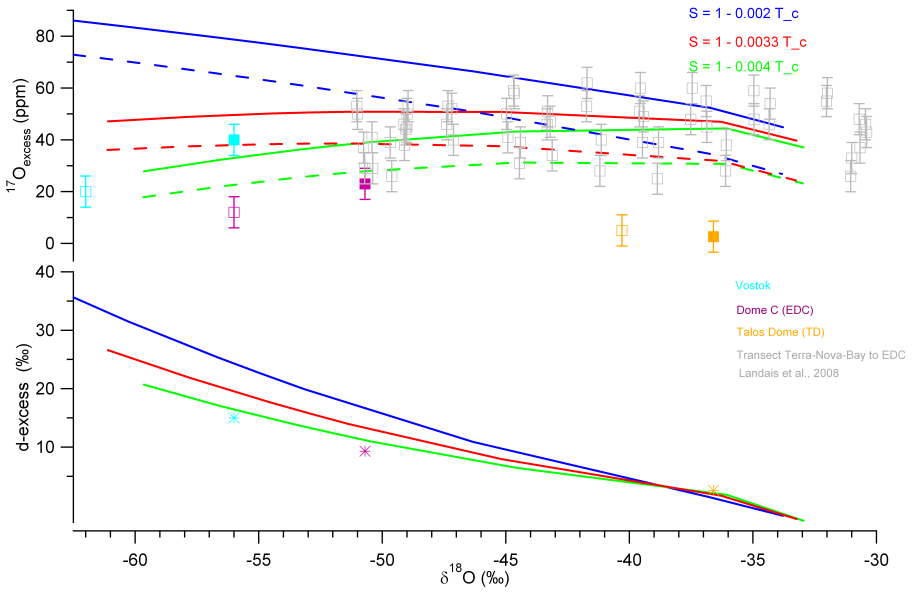

Fig. 3. Dependency of ^{17}O-*excess* (upper panel) and d-*excess* (lower panel) on supersaturation S as a function of δ^{18}O . The different coloured lines represent different S. The dashed lines represent S, but with 10 times more reevaporation (γ) of the liquid phase in the cloud. The filled symbols are the EH values and the empty ones are the LGM values of ^{17}O-*excess* (Error = ±6 ppm). The light grey dots are the data of the transect study from Terra Nova Bay to EDC (Landais et al., 2008). The dependency of d-*excess* with supersaturation S and the d-*excess* data (star-symbol) for EH (EPICA Members, 2004, Stenni et al., 2004, 2001 and Vimeux et al., 1999)

CPD
7, 1845–1886, 2011

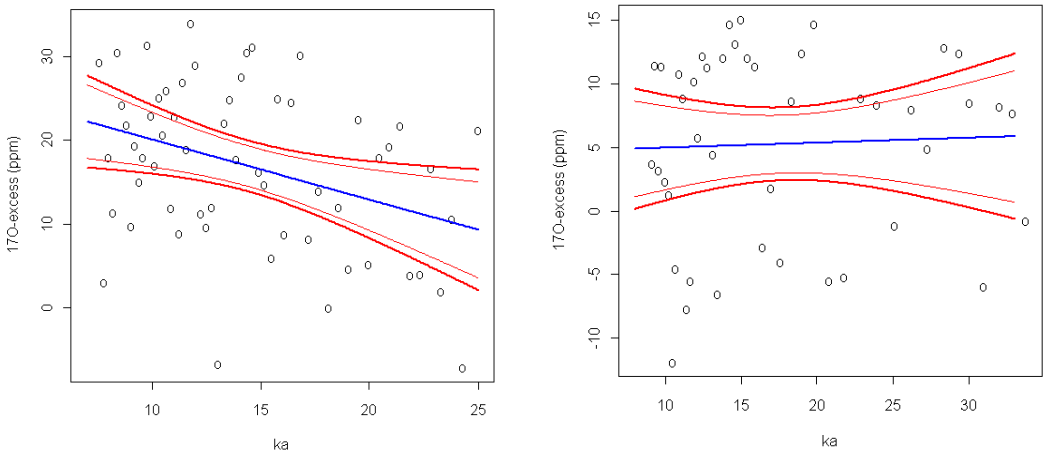

Fig. 4. Figure 4a (left for EDC) and b (right for TD) shows the results of linear regression analysis of the LGM-EH ^{17}O-*excess* data (blue lines). The red lines are the point-wise and simultaneous 95 % confidence bounds. See the Appendix A for the description of the method.

CPD
7, 1845–1886, 2011

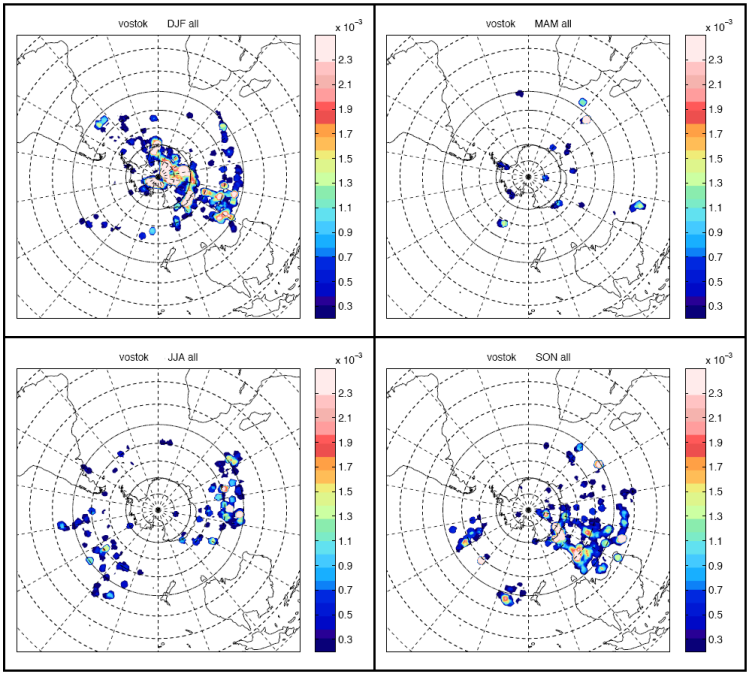

Fig. 5a. Moisture source diagnostics for Vostok: on the annual mean, moisture source longitude is 60° E. With 42° S, Vostok has the most northerly moisture source of the three sites. There are moisture sources stemming from the Pacific and during the months DJF, Vostok seems to be affected by moisture sources stemming from the interior of the continent.

CPD
7, 1845–1886, 2011

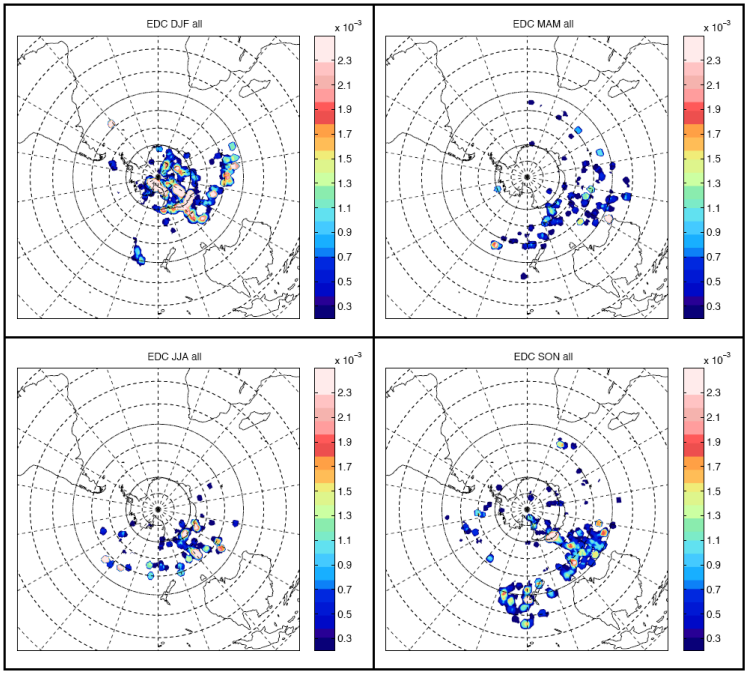

Fig. 5b. Moisture source diagnostics for EDC: on the annual mean, moisture source longitude is 60° E. The most northerly source is located at 44° S. Moisture is mainly coming from the western Indian Ocean but as for Vostok, it seems to have some sources stemming from the interior of the continent.

CPD
7, 1845–1886, 2011

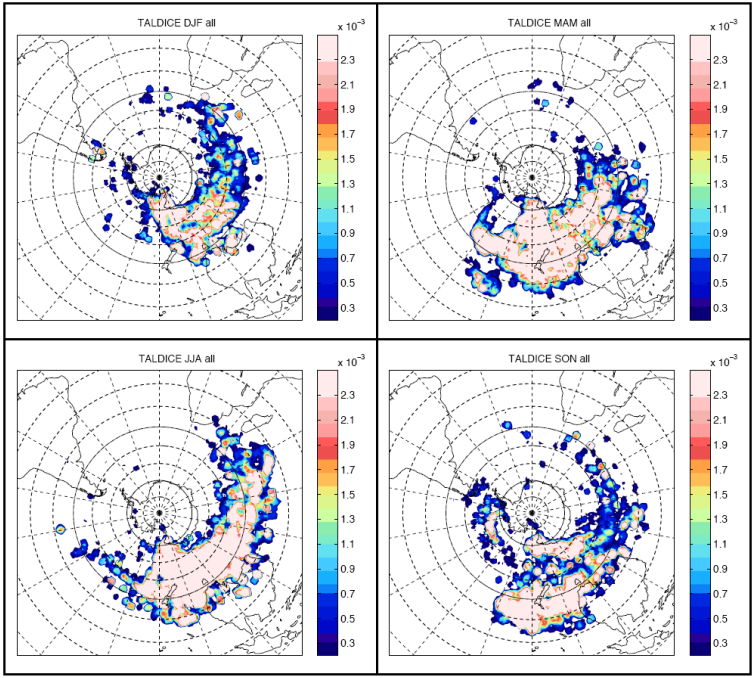

Fig. 5c. TD has more easterly moisture sources with annual mean moisture source longitude of 100° E. With 46° S, TD has the most southern moisture source of the three sites. TD shows a completely different pattern compared to Vostok and EDC, being a more low-altitude coastal site.

CPD
7, 1845–1886, 2011